ACS APPLIED MATERIALS & INTERFACES

Research Article

www.acsami.org

Confined Multiple Enzymatic (Cascade) Reactions within Poly(dopamine)-based Capsosomes

Leticia Hosta-Rigau,*[,†] Maria J. York-Duran,[†] Yan Zhang,[†] Kenneth N. Goldie,[‡] and Brigitte Städler*[,†]

[†]Interdisciplinay nanoscience center (iNANO), Aarhus University, 8000 Aarhus, Denmark

[‡]Center for Cellular Imaging & Nano Analytics, Biozentrum, University of Basel, CH-4058 Basel, Switzerland

Supporting Information

ABSTRACT: The design of compartmentalized carriers as artificial cells is envisioned to be an efficient tool with potential applications in the biomedical field. The advent of this area has witnessed the assembly of functional, bioinspired systems attempting to tackle challenges in cell mimicry by encapsulating multiple compartments and performing controlled encapsulated enzymatic catalysis. Although capsosomes, which consist of liposomes embedded within a polymeric carrier capsule, are among the most advanced systems, they are still amazingly simple in their functionality and cumbersome in their assembly. We report on capsosomes by embedding liposomes within a poly(dopamine) (PDA) carrier shell created in a solution-based single-step procedure. We demonstrate for the first time the potential of PDA-based capsosomes to act as artificial cell mimics by performing a two-enzyme coupled reaction in parallel with a single-enzyme conversion by encapsulating three different enzymes into separated liposomal compartments. In the former case, the enzyme uricase converts uric acid into hydrogen peroxide, CO_2 and allantoin, followed by the reaction of hydrogen peroxide with the reagent Amplex Ultra Red in the presence of the enzyme horseradish peroxidase to generate the fluorescent product resorufin. The parallel enzymatic catalysis employs the enzyme ascorbate oxidase to convert ascorbic acid into 2-*L*-dehydroascorbic acid.

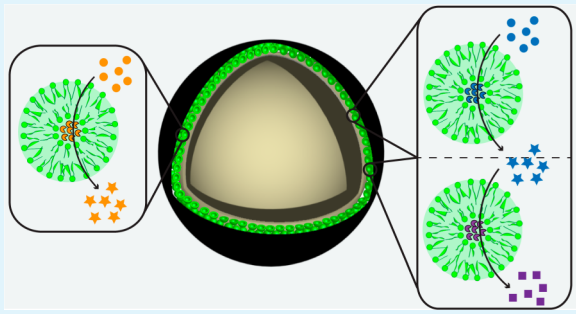

KEYWORDS: *liposomes, encapsulated catalysis, poly(dopamine), cascade reaction, capsosomes, uric acid*

INTRODUCTION

The assembly of multicompartment systems with a structure reminiscent of a biological cell is currently an emerging area of research that aims to create simplified synthetic cells. Artificial cells or synthetic cell mimics are envisioned to be an efficient tool in biomedicine with potential applications in the fields of drug delivery, (bio)sensing/diagnostics, or encapsulated (bio)-catalysis.[1,2] There is no life without compartmentalization, and living cells developed this strategy to temporally and spatially separate different cellular functions within specialized organelles to, for instance, separate highly reactive conditions, like the ones found in lysosomes and peroxisomes, which harm the rest of the cell, or to avoid undesired cross-reactions. For artificial cells mimic, the successful compartmentalization enables the use of external triggers to start/stop reactions within specific subunits or allows for the encapsulated enzymes and substrates to reach higher concentrations locally.

In recent years, considerable progress has been made in the design and assembly of single-compartment, functional, bioinspired systems that tackle the challenge of mimicking metabolism by performing encapsulated enzymatic reactions. These systems range from liposomes[3−5] or polymersomes[6,7] to polymer-based capsules,[8] and have been extensively reviewed in literature.[2,9] However, for the advanced design of artificial cell mimics, compartmentalization is essential, and few groups have succeeded in designing architectures containing several subunits entrapped within a larger carrier. In general, while subcompartments have the ability to protect fragile contents, e.g., to prevent enzymes from misfolding or denaturation by means of their sealed environment, the carrier supplies the system with the required structural integrity and should allow for the communication of the vehicle with the external milieu, a key feature to perform continuous cascade/parallel (enzymatic) reactions. Compartmentalized systems reported to date include single-component assemblies, in which both the carrier vehicle and the subcompartments are of the same nature, dual-composition systems, in which the carrier vehicle and the subcompartments are of different nature, and systems that encapsulate two intrinsically different subcompartments. Single-component assemblies are the most popular concept, and examples are vesosomes (liposomes within a carrier liposome),[10,11] two-compartment micelles,[12] polymer capsule(s) within a polymer capsule,[13−15] polymersomes within a polymersome,[16−22] or particles with concentric compartments fully made of biomolecules.[23] Dual-composition systems are far less common and they employ polymer hydrogel capsules

Received: May 5, 2014
Accepted: June 26, 2014
Published: June 26, 2014

containing different subunits, i.e., polymersomes,[24] cubosomes,[25] or liposomes. The latter case, termed capsosomes,[26,27] is the only system reported to date that progressed to such an extent that the encapsulation of two fundamentally different types of subcompartments (liposomes and polymer capsules) within the same carrier vessel was possible.[28] Although the building blocks of the reported multicompartment systems are quite diverse, only few single-component systems have demonstrated encapsulated enzymatic catalysis including liposomes within liposomes,[29] polymer capsule(s) within a polymer capsule,[30] and particles fully made of biomolecules.[23] When dual-composition systems are considered, reported functionality is even scarcer and, to the best of our knowledge, capsosomes are a single example. We demonstrated that capsosomes can be employed to preform triggered[31,32] and continuous[33] enzymatic conversions and a two-step enzymatic catalytic reaction.[34] We also demonstrated catalytic activity for capsosomes encapsulating both liposomes and polymeric capsules,[28] and that the catalytic activity of capsosomes was preserved for at least four subsequent cycles, i.e., the capsosomes could be reused.[32] However, all these approaches only employ the same enzyme encapsulated within the liposomal subunits. Despite the success of capsosomes in encapsulated biocatalysis or drug delivery,[35,36] their functionality remains very simple and their assembly cumbersome. In the latter case, although liposomes are easily prepared via self-assembly, the fabrication of the polymer carrier capsule relies on the labor-intensive sequential deposition of interacting polymer pairs (the layer-by-layer (LbL) technique[37]). Therefore, assembly of the carrier through a single-step, solution-based procedure would be highly beneficial.

Dopamine has received increasing attention due to its ability to self-polymerize onto virtually any type of substrate independent of material and shape forming poly(dopamine) (PDA).[38,39] Although the exact structure and the mechanism of the PDA deposition first reported by Lee et al.,[40] has not been fully elucidated yet,[22,27,41,42] PDA-coatings have been considered for a wide range of applications. Among the biggest advantages of LbL films is the possibility to fine-tune their properties depending on the choice of the building blocks. With the aim to develop PDA-based coatings with similar controllable diverse properties, dopamine has been conjugated to the reactants prior to the film deposition,[43−46] or PDA has been codeposited with polymers/biomolecules.[43,47−50] Templated PDA-based capsules have been assembled.[51−53] These capsules, although having no inherent toxicity toward cells,[51,53] have proven to entrap and release differently charged probing dyes at different pH,[54] and to efficiently encapsulate functional components such as magnetic nanoparticles, fluorescent quantum dots and a small antitumor compound.[53] The PDA-based capsules' potential as drug delivery vehicles by conjugating the antitumor drug doxorubicin to their surface making use of the chemical reactivity of PDA films toward thiols and amines, has also been demonstrated.[43] Furthermore, the ability of PDA-capsules to perform encapsulated catalysis has also been shown.[55] By incorporating three different enzymes at different locations, i.e., in the void of the capsule, and within and outside of the PDA membrane, a cascade reaction to convert starch into isomaltooligosacharide was performed.

Herein, we report on the assembly and characterization of capsosomes with simplified fabrication but considerably improved functional complexity. In particular, we (i) identify the optimal conditions to assemble structurally intact capsosomes using PDA as the carrier capsule, (ii) verify the capsosomes' functionality by performing a two-enzyme coupled cascade reaction toward the detection of uric acid, and (iii) perform multiple parallel reactions by encapsulating a third enzyme for the elimination of ascorbic acid during uric acid detection (Scheme 1).

Scheme 1. Schematic Illustration of the PDA-based Capsosomes Assembly[a]

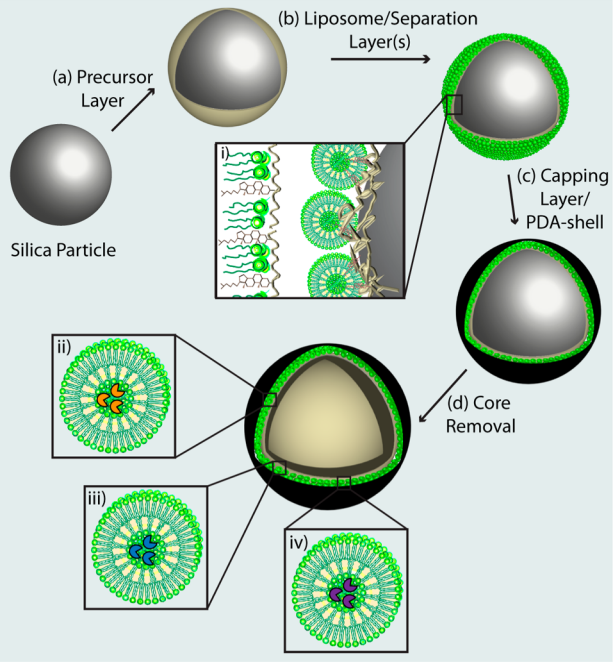

[a]A precursor polymer layer is deposited onto silica particles (a) followed by the deposition of (enzyme loaded) liposomes and separation polymer layers (b). The liposomes remain attached to the polymer by means of a noncovalent cholesterol anchoring (i). The assembly is then capped with an extra polymer layer and the PDA shell is assembled by the self-polymerization of dopamine (c) and PDA-based capsosomes containing liposomes loaded with three different enzymes (ii, iii, and iv) are obtained after core removal (d).

EXPERIMENTAL SECTION

Materials. Poly(*L*-lysine) (PLL, M_w 40−60 kDa), uricase (UR, from *Bacillus fastidiosus*, 33 kDa), horseradish peroxidase (HRP, peroxidase type VI from horseradish, 44 kDa), ascorbate oxidase (AO, from *Cucubrita* species, 140 kDa), uric acid, ascorbic acid, dopamine hydrochloride, sodium chloride (NaCl), tris(hydroxymethyl)-aminomethane (TRIS), sodium phosphate dibasic, sodium phosphate monobasic, and chloroform were purchased from Sigma-Aldrich. Amplex Ultra Red was obtained from Invitrogen. Silica particles (4.8 μm diameter) were purchased from Microparticles GmbH, Germany. Zwitterionic lipids, 1,2-dioleoyl-*sn*-glycero-3-phosphocholine (DOPC, phase transition temperature T_m= −20 °C) and fluorescent lipids 1-oleoyl-2-[6-[(7-nitro-2−1,3-benzoxadiazol-4-yl)amino]hexanoyl]-*sn*-glycero-3 phosphocholine (NBD-PC) were purchased from Avanti Polar Lipids, USA.

Four different buffers were used for the assembly: 10 mM or 100 mM TRIS with the pH adjusted to 7.0 or 8.5. These buffers are from now on referred to as TRIS-10 mM-pH7.0, TRIS-100 mM-pH7.0, TRIS-10 mM-pH8.5, and TRIS-100 mM-pH8.5. All buffer solutions were made with ultrapure water (Milli-Q gradient A 10 system, resistance 10MΩ cm, TOC < 4 ppb, Millipore Corporation, USA).

Poly(methacrylic acid)-*co*-(cholesteryl methacrylate) (PMA_c, M_w 33 kDa) was synthesized according to a previously published protocol.[56] The molecular weight of the PMA_c employed in this study is longer (M_w 33 kDa) than the PMA_c used in capsosomes previous reports (M_w 11.5 kDa).[57] Flow cytometry studies comparing liposomal loading depending on the PMA_c used, i.e., long vs short, demonstrate that the polymer length does not affect the amount of trapped liposomes (data not shown).

Liposome Formation. Unilamellar zwitterionic liposomes were prepared by evaporation of the chloroform of the lipid solution (2.5 mg) under nitrogen for 1 h, followed by hydration with 1 mL of TRIS-100 mM-pH7.0 containing 40 U of UR (L_{UR}), HRP (L_{HRP}), 200 U of AO (L_{AO}) or without containing any enzyme (L). For fluorescently labeled liposomes (L_F), 6 wt % of NBD-PC was added to the lipid solution. Each solution was extruded through 100 nm filters 11 times to obtain liposomes of monodisperse size. L_{AO} were extruded through 200 nm filters to favor AO encapsulation due to the large size of the enzyme.

Capsosome Assembly. A suspension of SiO_2 particles (5 wt %) in the required TRIS buffer was incubated with the polymer precursor layer, PLL (1 mg mL^{-1}, 10 min), and washed three times in TRIS buffer (100 g, 30 s) followed by the adsorption of a PMA_c layer if needed (0.7 mg mL^{-1}, 10 min), washed three times in TRIS buffer and suspended in a liposome solution (2.5 mg mL^{-1}, 50 min), washed three times in TRIS, and incubated in a PMA_c solution again (0.7 mg mL^{-1}, 15 min). When the deposition of a second liposome layer was required, a PMA_c (0.7 mg mL^{-1}, 15 min) separation layer was adsorbed, washed three times in TRIS, followed by the absorption of a second liposome deposition step at the desired concentration (from 0.125 to 2.5 mg mL^{-1}, 50 min). The samples were then washed three times in TRIS followed by the adsorption of a PMA_c capping layer (0.7 mg mL^{-1}, 15 min).

When employing fluorescent lipids, the samples were covered with aluminum foil to avoid the exposure of the fluorescent dyes to light and possible photobleaching. When adsorbing enzyme loaded liposomes (L_{UR}, L_{HRP}, or L_{AO}), the lipid concentration in both liposomal deposition steps was 2.0 mg mL^{-1}, because that is the concentration that ensures fully saturation of the particles' surface (Supporting Information, Figure S5). When fluorescently labeled liposomes are adsorbed, the lipid concentration during the first liposomal deposition step was 2.0 mg mL^{-1}, whereas for the second liposomal deposition step, the lipid concentration ranged from 0.125 to 2.5 mg mL^{-1}. After the PMA_c capping layer is absorbed, the core–shell particles were washed in TRIS-10 mM-pH8.5 and the PDA shell was deposited by incubating them in a dopamine solution (8 mg mL^{-1} in TRIS-10 mM-pH8.5) for ~16 h. After the incubation time, the core–shell particles where washed three times in a TRIS solution (TRIS 10 mM, 150 mM NaCl, pH 7.4). PDA-based capsosomes were formed by dissolving the silica core particles using a 2 M hydrofluoric acid (HF)/8 M ammonium fluoride (NH_4F) solution at pH 5 for 2 min, followed by multiple centrifugation (1680*g*, 5 min) washing cycles in Milli-Q water (MQ).

Dynamic Light Scattering (DLS). The size and polydispersity (PD) of the liposomes was determined by diluting 30–50 μL of sample solution in ~700 μL of MQ prior to measuring in a DLS instrument (Zeta-sizer nano, Malvern Instruments) using a material refractive index of 1.590 and a dispersant (water at 25 °C) refractive index of 1.330. Liposomes extruded through a 100 or 200 nm membrane were found to have a diameter ~120 nm or ~240 nm, respectively, with a PD < 0.15.

Quartz Crystal Microbalance with Dissipation Monitoring (QCM-D). QCM-D measurements (Q-sense E4, Sweden) were used to analyze the liposome and polymer deposition on planar silica substrates depending on the polymer precursor layer (PLL or PLL/PMA_c) and the used TRIS buffer condition. Silica-coated crystals (QSX300, Q-sense) were cleaned by immersion in a 2 wt % sodium dodecyl sulfate solution overnight, rinsing with Milli-Q water, blow-dried with N_2, followed by exposure to UV/ozone for 20 min before being mounted into the liquid-exchange chambers of the instrument. The frequency and dissipation measurements were monitored at 23 ± 0.02 °C. When a stable baseline in the buffer solution was achieved, a PLL solution (1 mg mL^{-1}) was introduced into the measurement chamber, left to adsorb onto the crystal and after surface saturation, the chamber was rinsed to remove the excess polymer. If required, PMA_c (0.7 mg mL^{-1}) was added as the next polymer layer and upon surface saturation, the chamber was rinsed. This way, the PLL or PLL/PMA_c precursor layers were deposited. The resulting polymer-coated surface was then exposed to L (2.5 mg mL^{-1}) and left to incubate until the surface was saturated. The liposome solution was replaced with buffer solution and the film assembly was continued by adsorbing a PMA_c separation layer (0.7 mg mL^{-1}). When the surface was saturated, the chambers were washed with buffer solution and exposed to a second L solution (2.5 mg mL^{-1}). Upon surface saturation and buffer rinsing, the assembly was capped with a PMA_c (0.7 mg mL^{-1}) layer and rinsed with buffer. After the buffer was changed to TRIS-10 mM-pH8.5, the PDA layer was deposited using 10 mg mL^{-1} dopamine in TRIS-10 mM-pH8.5. During this deposition step, the pump was set to 50 μL min^{-1} and after 30 min the dopamine solution was replaced with a freshly prepared one, to ensure that enough monomers were available for the deposition of the PDA. Normalized frequencies and dissipation values using the third harmonics are presented.

Flow Cytometry. The fluorescence of the particles was analyzed by flow cytometry before and after core removal. BD Accuri C6 flow cytometer using an excitation wavelength of 488 nm and emission detection of 530 nm was used to measure the fluorescence intensity of the core–shell particles or capsosomes containing L_F. At least 20 000 particles were analyzed in each experiment and at least two independent experiments were performed.

Differential Interference Contrast (DIC) Microscopy. DIC images of capsosomes were taken with an inverted Zeiss microscope Axio Observer Z1 (Zeiss, Germany) equipped with a DIC slider, the corresponding filter sets and a 63× oil immersion objective.

Confocal Laser Scanning Microscopy (CLSM). Capsosomes containing fluorescently labeled liposomes were imaged with an Axiovert microscope coupled to an LSM 700 confocal laser scanning module (Zeiss, Germany).

Transmission Electron Microscopy (TEM). The capsosomes were also visualized using TEM by adsorbing 4 μL of the capsule suspension onto a carbon film mounted on 300 mesh copper grids (Quantifoil Micro Tools GmbH, Jena, Germany) for 5 min. The grid surface was rendered hydrophilic by glow discharge in a reduced atmosphere of air for 10 s prior to adsorption. The grid was blotted and left to air dry. TEM images of the capsules were acquired digitally using a Philips CM10 microscope (FEI, Eindhoven, The Netherlands) fitted with a 2k × 2k side-mounted CCD Camera (Olympus SIS, Münster, Germany).

Atomic Force Microscopy (AFM). 1–2 μL of the capsosome solution was dried on a piece of silica wafer and visualized in air using tapping mode AFM (Nanowizard 2, JPK Germany) using NCH cantilever (NanoWorld).

Enzymatic Reactions. *Kinetics of Enzymatic Conversion of Uric Acid in UR and HRP Loaded Capsosomes.* A suspension of 2.25 × 10^5 capsosomes or capsules per μL loaded with an equal mixture of L_{UR} and L_{HRP} for capsosomes or free UR and HRP for the capsules, was allowed to interact with a solution 50 μM of Amplex Ultra Red and 10 μM of uric acid in phosphate buffer (100 mM, pH 7.0) at 37 °C. The increase of the fluorescent product resorufin was followed over time through monitoring fluorescence readings at an excitation and an emission wavelength of 550 and 580 nm, respectively, using an Enspire PerkinElmer plate reader. The results were normalized to the resorufin's fluorescence intensity after 22 h of reaction.

Enzymatic Conversion of Several Concentrations of Uric Acid in UR and HRP Loaded Capsosomes. A suspension of 2.0 × 10^5 capsosomes or capsules per μL loaded with an equal mixture of L_{UR}, L_{HRP}, and empty L for capsosomes or free UR and HRP for the capsules, was allowed to interact with a solution 50 μM of Amplex Ultra Red and several concentrations of uric acid (ranging from 10 to 100 μM) in phosphate buffer (100 mM, pH 7.0) at 37 °C. Empty liposomes were employed because we aimed to obtain a high signal to perform the next experiment in which liposomes encapsulating AO

(L_{AO}) will replace the empty ones. The fluorescence intensity of resorufin was measured after 3 h of reaction using an excitation and an emission wavelength of 550 and 580 nm, respectively, using the multi plate reader. The results were normalized to the resorufin's fluorescence intensity when employing a concentration 100 μM of uric acid.

Ascorbate Oxidase Reaction. A suspension of 2.0 × 10^5 capsosomes per μL loaded with an equal mixture of L_{UR}, L_{HRP}, and empty L or an equal mixture of L_{UR}, L_{HRP}, and L_{AO}, was allowed to interact with a solution 100 μM of ascorbic acid in phosphate buffer (100 mM, pH 7.0) at 37 °C for 3 h followed by the addition of uric acid and Amplex Ultra Red at final concentrations of 100 and 50 μM, respectively. The increase of the fluorescent product resorufin was followed over time through monitoring fluorescence readings at an excitation and an emission wavelength of 550 and 580 nm, respectively, using the multi plate reader.

RESULTS AND DISCUSSION

Assembly. The goal of this part is to compare the liposome deposition depending on the used polymer precursor layer(s) PLL or PLL/PMA_c and the buffer conditions. Although we previously identified PLL and PLL/PMA_c as suitable precursor layer(s), the same assembly buffer was always used, namely 10 mM 2-[4-(2-hydroxyethyl)piperazin-1-yl]ethanesulfonic acid, 150 mM NaCl adjusted to pH 7.4. Because we were aiming to use PDA to assemble the carrier capsules, we investigated if the same buffer solution could be used for the entire assembly and to what extent the TRIS concentration and the pH affected the amount of deposited liposomes on planar and colloidal substrates. When the first liposome deposition step is considered, PLL as a precursor layer allowed for the deposition of similarly high amounts of liposomes independent of the used buffer. For PLL/PMA_c precursor layers, only TRIS-100 mM-pH7.0(8.5) buffer facilitated the deposition of liposomes on both planar and colloidal substrates. (For more details, see the Supporting Information, Figure S1). Further, only the use of TRIS-100 mM-pH7.0(8.5) buffers allowed for the liposome deposition during a second adsorption step. (For more details, see the Supporting Information, Figure S2).

With the aim to advance the assembly of the capsosomes' shell, which, so far, has mainly been deposited using the LbL technique employing the polymer pair poly(*N*-vinylpyrrolidone) and thiolated poly(methacrylic acid),[58] we considered PDA to assemble the carrier vehicle in a single-step. The PDA deposition is one final step, which replaces the so far used sequential deposition of at least eight layers of thiolated poly(methacrylic acid) and poly(vinylpyrrolidone) followed by a cross-linking step. The PDA adsorption would therefore considerably facilitate the assembly process. Frequency changes (Δf) (Figure 1a) and frequency changes (ΔD) (Supporting Information, Figure S3) of the crystals due to the entire film built up were monitored by QCM-D in TRIS-100 mM-pH7.0(8.5) buffer including the deposition of the PDA for 1 h in the last step. (The short PDA deposition time was chosen due to practical reasons, especially to avoid potential clogging of the QCM-D chambers due to the PDA deposition). Independent of the used buffer solution during the liposome deposition steps, the adsorption of the PDA was confirmed without rupture or displacement of the liposomes. When the crystal was precoated with liposomes using TRIS-100 mM-pH7.0 buffer as compared to TRIS-100 mM-pH8.5 buffer, higher Δf and similar ΔD of the crystals due to the initial PDA deposition was observed. This might indicate that a more hydrated (or less dense) PDA film was deposited in the former

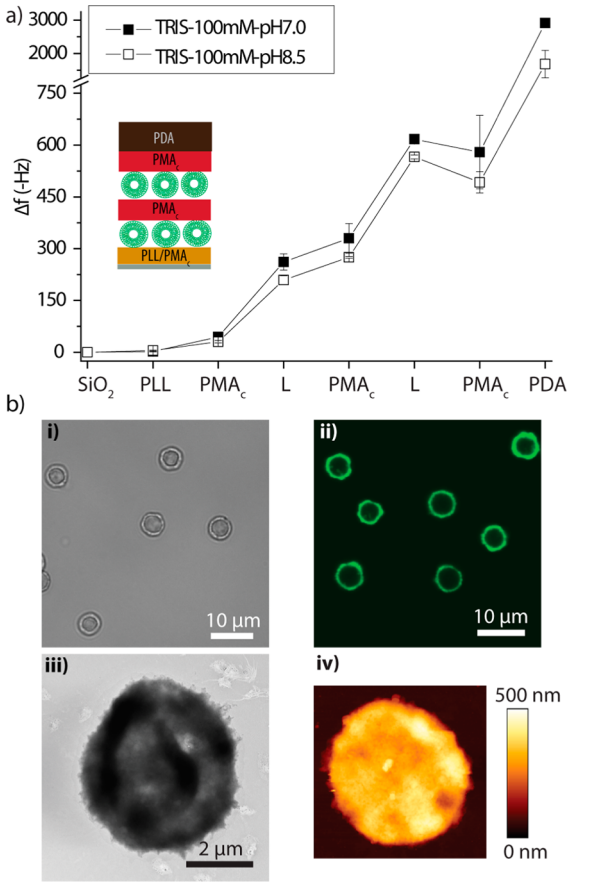

Figure 1. (a) Change in frequency Δf of a QCM-D crystal up on the film built up using two liposome deposition steps including the adsorption of the PDA as the last step using TRIS100 mM-pH7.0(8.5) as the buffer condition. (b) Structural characterization of capsosomes by several microscopy techniques: DIC (i), CLSM (ii), TEM (iii), and AFM (iv) images of PLL/PMA_c/L_F/PMA_c/L_F/PMA_c/PDA assembled in TRIS-100 mM-pH7.0 are shown.

case. We speculate that the pH could affect the amount of TRIS molecules predeposited in the liposome-containing film, leading to different PDA adsorption properties, because TRIS molecules have previously been proposed to be involved in the PDA formation.[42] Results using colloidal substrates and flow cytometry as readout method supported the hypothesis that the deposited PDA coating was different depending on the assembly conditions of the underlying layers. (For more details, see the Supporting Information, Figure S4).

Due to consideration regarding biological relevant pH for enzymes to be encapsulated into the liposomes and the potentially more hydrated PDA carrier capsules, which might facilitate the transport of substrate/product across the polymer membrane, we decided to only consider PLL/PMA_c/L/PMA_c/L/PMA_c/PDA films assembled in TRIS-100 mM-pH7.0. In a next step, the silica core was removed using buffered HF solution. Buffered HF (~pH 5) was used in order to avoid exposure of encapsulated enzymes to highly acidic condition. The core was removed in order to demonstrate that PDA provides enough structural integrity to allow for free-standing polymer/liposome assemblies, which would also be amendable for using liposomal subunits "free-floating" in the capsosome's void.[33] In addition, for many biomedical applications, it might be beneficial to remove the core because silica is (i) nondegradable, (ii) adds weight to the assembly, which might

affect its ability to remain in suspension, or (iii) likely to affect the interaction with cells and tissue due to its nondeformability among others. The structural integrity of yielded capsosomes was visualized by several microscopy techniques (Figure 1b). Differential interference contrast (DIC) images demonstrated that the capsosomes were intact, discrete, monodisperse, and maintained the round shape of the template silica particles (Figure 1bi). Fluorescent confocal scanning laser microscopy images revealed that the liposomes where homogeneously distributed along the PDA membrane as shown by the regular green fluorescence (Figure 1bii). Transmission electron microscopy (TEM, Figure 1biii) and atomic force microscopy (AFM, Figure 1biv) images further support the assembly of capsosomes due to the particle-like much denser structure in contrast to the creases and folds of polymer capsules without liposomes. The shell thickness of this type of capsosomes was measured from cross-sectional profiles of AFM height images and found to be 128 ± 1 nm. We would also like to note that by varying the liposome concentration during the adsorption step, the amount of adsorbed liposomes could be controlled. (For details, see the Supporting Information, Figure S5).

Enzymatic Cascade Reaction. Biological cells operate by performing multiple (cascade) reactions within spatially separated and confined subcompartments, the cell organelles. However, initially, the reported systems with ability to perform coupled enzymatic reactions consist of capsules/particles with double- or multishelled architectures in an onion-like fashion. Kreft et al.[30] pioneered the performance of two-enzyme-coupled reactions within shell-in-shell polyelectrolyte capsules, a concept that was pushed further by Bäumler et al.,[23] who conducted a three-enzyme cascade reaction by encapsulating three different enzymes in three concentric compartments. In the past few years, multishelled structures performing multi-enzyme reactions have spurred increasing interest.[59] The aforementioned reports are of utmost interest and important in their own rights because, in nature, some cells or organelles possess double membranes, e.g., the mitochondria, in which several of the enzymes for the citric acid cycle are located in the intermembrane space. However, the vast majority of cells have multiple subcompartments situated in different areas within their interior arranged in a nonconcentrically manner. To this end, two recent publications using polymersomes within polymersome architectures have demonstrated the ability to perform enzymatic cascade reactions in this multicompartment arrangement.[21,22]

With the aim to advance the functional complexity of capsosomes, we report, for the first time, an encapsulated cascade reaction within this multicompartment system. As proof of concept, we chose to perform a cascade enzymatic reaction toward uric acid detection. Quantitative analysis of uric acid in body fluids, e.g., urine or blood, is very important in the diagnosis and medical management of various diseases. Abnormal uric acid levels may result from leukemia, toxemia of pregnancy, polycythemia, impaired renal function, or gout disease.[60−62] A number of colorimetric assays for the detection of uric acid in biological samples have been developed by coupling the uricase (UR) reaction with the peroxidase-catalyzed oxidation of a chromophore by hydrogen peroxide (H_2O_2). This is a simple, sensitive and specific method, which does not require an expensive apparatus.[62,63] UR catalyzes the conversion of uric acid to allantoin, H_2O_2, and carbon dioxide (CO_2). Next, H_2O_2 reacts in the presence of horseradish peroxidase (HRP) with Amplex Ultra Red reagent to generate the red-fluorescent oxidation product resorufin, which can be detected by fluorescence spectroscopy at an excitation and an emission wavelength of ∼570 and ∼585 nm, respectively. Because capsosomes have the inherent ability to immobilize multienzymes in the liposomal subunits, we encapsulated UR and HRP in the liposomal subunits and performed a continuous cascade reaction by converting the analyte uric acid. An equal mixture of liposomes containing UR (L_{UR}) or HRP (L_{HRP}) was employed for the capsosomes assembly. Unsaturated zwitterionic liposomes were chosen for the capsosomes' assembly due to their low phase-transition temperature (T_m = −20 °C), because that allows performing enzymatic reactions without the need of an external trigger. Due to the high permeability of the liposomal membrane at room temperature, uric acid is expected to be able to permeate through the lipid membrane and to be converted by UR into allantoin and H_2O_2 (Figure 2ai). The latter, together with the small probe Amplex Ultra Red, will be converted by HRP into the fluorescent product resorufin (Figure 2aii).

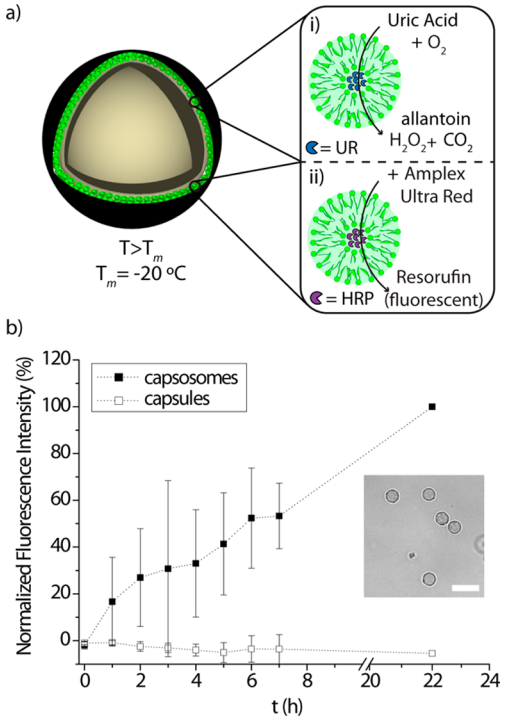

Figure 2. Enzymatic cascade reaction. (a) Schematic illustration of the enzymatic cascade reaction performed in capsosomes. At $T > T_m$, the substrate uric acid in the presence of O_2 is able to permeate through the liposomes membrane and be converted by the enzyme uricase (UR) into H_2O_2, CO_2, and allantoin (i). H_2O_2 reacts with Amplex Ultra Red reagent in the presence of horseradish peroxidase (HRP) to generate the fluorescent product resorufin (ii). (b) Reaction kinetics of capsosomes containing an equal mixture of liposomes loaded with UR and HRP, respectively (black squares), in comparison to capsules assembled by adsorbing free enzymes (white squares). DIC image of capsosomes after 22 h of reaction (inset). The scale bar is 10 μm.

The kinetics of the enzymatic conversion was followed at a concentration of 10 μM uric acid and 50 μM Amplex Ultra Red reagent in 100 mM phosphate buffer (pH 7.0) using a concentration of 2.25 × 10^5 capsosomes per μL (Figure 2b). The results were normalized to the resorufin's fluorescence intensity after 22 h of reaction. The resofurin fluorescence

steadily increased for the first 6−7 h, giving rise to 50% conversion of the total conversion measured after 22 h. As a control, capsules assembled by exposing the particles to the free enzymes in solution instead of the enzyme loaded liposomes, were used. We would like to note that QCM-D experiments revealed that the free enzymes did not adsorb to a PLL/PMA_c precoated crystal, highlighting the importance of the use of liposomes as subunits to carry the enzymes (results not shown). Further, this control experiment strongly implies that the liposomes remain intact after core removal, as previously demonstrated.[31,33,34] If the liposomes would have been destroyed during the HF treatment, the enzymes would likely have been removed during the subsequent washing cycles and no enzymatic conversion would have been observed. In agreement with this finding, the fluorescent product was only detected in the capsosome samples (Figure 2b, black squares), but not in the control (Figure 2b, white squares), demonstrating that the liposomes were required to ensure the functional presence of the enzymes. After 22 h of enzymatic reaction, the capsosomes preserved their structural integrity (Figure 2b, inset). The fluorescence intensity of the enzymatic conversion after 3 h at a concentration of 10 μM uric acid and 50 μM Amplex Ultra Red reagent in 100 mM phosphate buffer (pH 7.0) using a concentration of 3×10^5 capsosomes or core−shell particles per μL was also measured to confirm that there was no significant reduction of enzyme activity after core removal (Supporting Information, Figure S6). We would like to note that although the detection times used here were relatively large (>1 h), they could be reduced by, e.g., increasing the number of entrapped liposomes per capsosome, which would increase the enzyme concentration, or by concentrating the number of capsosomes per volume.

With the aim to assess the effect of the initial uric acid concentration on the encapsulated enzymatic cascade reaction, we incubated the capsosomes with different amount of this analyte for 3 h and measured the conversion. The normalized fluorescence intensity of the fluorescent reaction product resorufin is plotted in dependence of the uric acid concentration (Figure 3a). The results were normalized to resorufin's fluorescence intensity when employing 100 μM uric acid. Concentrations of uric acid as high as 100 μM could be used, and the capsosomes preserved their integrity for all the tested concentrations (Figure 3b). However, upon incubation of the capsosomes with 300 μM uric acid, loss of their spherical shape and aggregation was observed (data not shown). We attribute those results to a potential interaction of uric acid with the PDA shell, which would further indicate that the PDA structure could predominantly consist on noncovalent bonds.[41] This drawback could likely be overcome by using dopamine-modified cross-linkers and/or the addition of protective layer(s).

Multiple Enzymatic Reactions. Biological cells are able to perform simultaneous multiple (cascade) reactions spatially separated, but this aspect still presents a significant challenge in cell mimicry. Here, we aim to push the limits of encapsulated catalysis further by conducting an additional enzymatic conversion in parallel to the above-described cascade reaction using capsosomes. We make use of the fact that certain compounds can interfere with the uric acid detection. In body fluids, ascorbic acid is one of the main interfering substances due to its strong reducing activity, which disturbs when using oxidase-based chromogenic detection.[64] The enzyme ascorbate oxidase (AO) is commonly added to preserve the chromophore

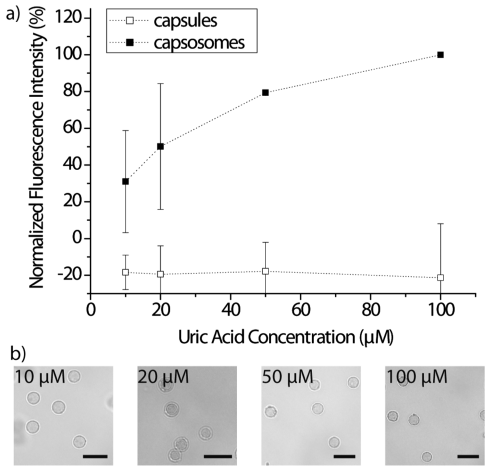

Figure 3. Uric acid concentration dependent conversion. (a) Normalized fluorescence intensity of resorufin reaction product depending on the uric acid concentration measured after 3 h of reaction for capsosomes loaded with uricase (UR) and horseradish peroxidase (HRP) within their liposomal compartments (black squares) in comparison to capsules assembled in a similar way but adsorbing the free enzymes instead of the loaded liposomes (white squares). (b) DIC images of capsosomes after 3h of reaction at different concentrations of uric acid. The scale bars are 10 μm.

from reduction by elimination of the ascorbic acid, which will be converted to 2-*L*-dehydroascorbic acid.[63,64] We compare capsosomes loaded with equal amounts of L_{UR}, L_{HRP}, and empty liposomes (L) vs capsosomes loaded with equal amounts of L_{UR}, L_{HRP}, and AO loaded liposomes (L_{AO}) in their ability to convert uric acid into the fluorescent probe via enzymatic conversion in the presence of ascorbic acid. In the latter case, the presence of AO should eliminate the ascorbic acid, leading to more efficient uric acid detection i.e., higher amount of fluorescent product (Figure 4a). Considering that the concentration of ascorbic acid in serum of a healthy subject is between 10 and 100 μM,[65] a suspension of 2.0×10^5 capsosomes per μL was incubated in a solution of 100 μM ascorbic acid and 100 μM uric acid followed by the addition of Amplex Ultra Red. The fluorescence intensity reading over time for capsosomes containing L_{AO} (Figure 4b, black squares) was higher that the fluorescence intensity reading of capsosomes containing L instead of L_{AO} (Figure 4b, white circles). This result impressively demonstrated that three enzymes could be entrapped within the same capsosome, exhibiting their expected function. We would like to note that the enzymatic conversion was measured for max 3 h, because we aimed to demonstrate the activity of multiple enzymes, which was convincingly done after this time. We believe that the mean fluorescence would increase with increasing time as observed in Figure 2b. This feasibility study showed, for the first time, multiple (cascade) reactions taking place simultaneously within a confined synthetic compartmentalized structure.

CONCLUSIONS

In summary, we have advanced capsosomes by employing a less cumbersome assembly approach of the carrier capsules while enhancing the complexity of their functionality for encapsulated catalysis. We assembled the carrier shell in a single-step by the spontaneous deposition of PDA yielding nonaggregated intact capsosomes. We identified a condition (buffer and precursor/separation layer(s)) that allowed for the highest liposome

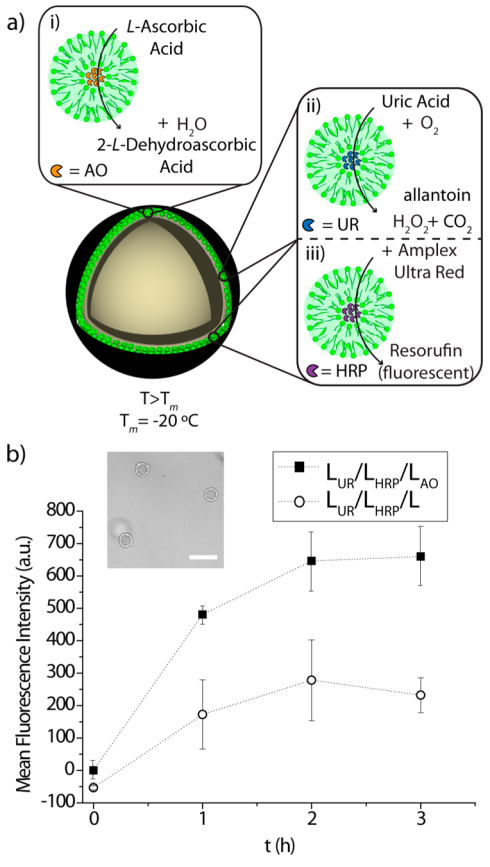

Figure 4. Multiple enzymatic reactions. (a) Schematic illustration of the multiple (cascade) enzymatic reactions performed in capsosomes. At $T > T_m$, ascorbic acid crosses the membrane of the liposomal subunits and can be converted by ascorbate oxidase (AO) into the product 2-*L*-dehydroascorbic acid (i). Simultaneously, the substrate uric acid, in the presence of O_2, is able to permeate through the liposomes membrane and be converted by the enzyme uricase (UR) into H_2O_2, CO_2, and allantoin (ii). H_2O_2 reacts with Amplex Ultra Red reagent in the presence of horseradish peroxidase (HRP) to generate the fluorescent product resorufin (iii). (b) Reaction kinetics of capsosomes containing an equal mixture of liposomes loaded with UR (L_{UR}), HRP (L_{HRP}), and AO (L_{AO}), respectively (black squares), in comparison to capsosomes loaded with an equal mixture of L_{UR}, L_{HRP}, and empty liposomes (L) (white circles). DIC image of capsosomes containing L_{UR}, L_{HRP}, and L_{AO} after 3 h of reaction (inset). The scale bar is 10 μm.

encapsulation by using PLL/PMA_c as precursor layers, PMA_c as separation layers, and TRIS-100 mM-pH7.0 as the buffer condition during the assembly. Further, we showed that three different enzymes, UR, HRP, and AO, can be encapsulated within the liposomal subcompartments. These assemblies are among the first ever used (nonconcentric) compartmentalized systems that could be successfully employed in encapsulated catalysis performing multiple reactions in parallel. These findings are substantially contributing to the advancement of cell mimicry applicable as both therapeutic carriers or biosensors.

■ ASSOCIATED CONTENT

Supporting Information

Optimization of the liposome deposition steps depending on the used buffer solution, dissipation changes of QCM-D measurements, PDA deposition onto colloids, lipid concentration dependence on the amount of deposited liposomes, and the comparison of the enzymatic activity in core−shell particles and capsosomes. This material is available free of charge via the Internet at http://pubs.acs.org.

■ AUTHOR INFORMATION

Corresponding Authors

*B. Städler. E-mail: bstadler@inano.au.dk.

*L. Hosta-Rigau. E-mail: leticia@inano.au.dk.

Notes

The authors declare no competing financial interest.

■ ACKNOWLEDGMENTS

This work was supported by a Marie Curie individual fellowship (L. H.-R.) and the Carlsberg foundation, Denmark. We thank Associate Prof. R. Meyer (iNANO, Aarhus University, Denmark) for access to the AFM and CLSM and Associate Prof. A. Zelikin (Department of Chemistry, Aarhus University) for access to the DLS, plate reader, flow cytometer, and microscope.

■ REFERENCES

(1) Chandrawati, R.; Caruso, F. Biomimetic Liposome- and Polymersome-Based Multicompartmentalized Assemblies. *Langmuir* **2012**, *28*, 13798−13807.

(2) Marguet, M.; Bonduelle, C.; Lecommandoux, S. Multicompartmentalized Polymeric Systems: towards Biomimetic Cellular Structure and Function. *Chem. Soc. Rev.* **2013**, *42*, 512−529.

(3) Walde, P. Building Artificial Cells and Protocell Models: Experimental Approaches with Lipid Vesicles. *BioEssays* **2010**, *32*, 296−303.

(4) Noireaux, V.; Libchaber, A. A Vesicle Bioreactor as a Step Toward an Artificial Cell Assembly. *Proc. Natl. Acad. Sci. U. S. A.* **2004**, *101*, 17669−17674.

(5) Cans, A. S.; Wittenberg, N.; Karlsson, R.; Sombers, L.; Karlsson, M.; Orwar, O.; Ewing, A. Artificial Cells: Unique Insights into Exocytosis Using Liposomes and Lipid Nanotubes. *Proc. Natl. Acad. Sci. U. S. A.* **2003**, *100*, 400−404.

(6) LoPresti, C.; Lomas, H.; Massignani, M.; Smart, T.; Battaglia, G. Polymersomes: Nature Inspired Nanometer Sized Compartments. *J. Mater. Chem.* **2009**, *19*, 3576−3590.

(7) Meng, F. H.; Engbers, G. H. M.; Feijen, J. Biodegradable Polymersomes as a Basis for Artificial Cells: Encapsulation, Release and Targeting. *J. Controlled Release* **2005**, *101*, 187−198.

(8) Price, A. D.; Zelikin, A. N.; Wang, Y.; Caruso, F. Triggered Enzymatic Degradation of DNA within Selectively Permeable Polymer Capsule Microreactors. *Angew. Chem., Int. Ed.* **2009**, *48*, 329−332.

(9) Peters, R. J. R. W.; Louzao, I.; van Hest, J. C. M. From Polymeric Nanoreactors to Artificial Organelles. *Chem. Sci.* **2012**, *3*, 335−342.

(10) Kisak, E. T.; Coldren, B.; Evans, C. A.; Boyer, C.; Zasadzinski, J. A. The Vesosome—A Multicompartment Drug Delivery Vehicle. *Curr. Med. Chem.* **2004**, *11*, 199−219.

(11) Mishra, V.; Mahor, S.; Rawat, A.; Dubey, P.; Gupta, P. N.; Singh, P.; Vyas, S. P. Development of Novel Fusogenic Vesosomes for Transcutaneous Immunization. *Vaccine* **2006**, *24*, 5559−5570.

(12) Thunemann, A. F.; Kubowicz, S.; von Berlepsch, H.; Mohwald, H. Two-Compartment Micellar Assemblies Obtained via Aqueous Self-Organization of Synthetic Polymer Building Blocks. *Langmuir* **2006**, *22*, 2506−2510.

(13) Pekarek, K. J.; Jacob, J. S.; Mathiowitz, E. Double-Walled Polymer Microspheres for Controlled Drug-Release. *Nature* **1994**, *367*, 258−260.

(14) De Geest, B. G.; De Koker, S.; Immesoete, K.; Demeester, J.; De Smedt, S. C.; Hennink, W. E. Self-Exploding Beads Releasing Microcarriers. *Adv. Mater.* **2008**, *20*, 3687−3691.

(15) Kulygin, O.; Price, A. D.; Chong, S. F.; Städler, B.; Zelikin, A. N.; Caruso, F. Subcompartmentalized Polymer Hydrogel Capsules with Selectively Degradable Carriers and Subunits. *Small* **2010**, *6*, 1558−1564.
(16) Marguet, M.; Edembe, L.; Lecommandoux, S. Polymersomes in Polymersomes: Multiple Loading and Permeability Control. *Angew. Chem., Int. Ed.* **2012**, *51*, 1173−1176.
(17) Chiu, H. C.; Lin, Y. W.; Huang, Y. F.; Chuang, C. K.; Chern, C. S. Polymer Vesicles Containing Small Vesicles within Interior Aqueous Compartments and pH-Responsive Transmembrane Channels. *Angew. Chem., Int. Ed.* **2008**, *47*, 1875−1878.
(18) Fu, Z.; Ochsner, M. A.; de Hoog, H.-P. M.; Tomczak, N.; Nallani, M. Multicompartmentalized Polymersomes for Selective Encapsulation of Biomacromolecules. *Chem. Commun.* **2011**, *47*, 2862−2864.
(19) Kim, S.-H.; Shum, H. C.; Kim, J. W.; Cho, J.-C.; Weitz, D. A. Multiple Polymersomes for Programmed Release of Multiple Components. *J. Am. Chem. Soc.* **2011**, *133*, 15165−15171.
(20) Shum, H. C.; Zhao, Y.-j.; Kim, S.-H.; Weitz, D. A. Multicompartment Polymersomes from Double Emulsions. *Angew. Chem., Int. Ed.* **2011**, *50*, 1648−1651.
(21) Siti, W.; de Hoog, H.-P. M.; Fischer, O.; Shan, W. Y.; Tomczak, N.; Nallani, M.; Liedberg, B. An Intercompartmental Enzymatic Cascade Reaction In Channel-Equipped Polymersome-In-Polymersome Architectures. *J. Mater. Chem. B* **2014**, *2*, 2733−2737.
(22) Peters, R. J. R. W.; Marguet, M.; Marais, S.; Fraaije, M. W.; van Hest, J. C. M.; Lecommandoux, S. Cascade Reactions in Multicompartmentalized Polymersomes. *Angew. Chem., Int. Ed.* **2014**, *53*, 146−150.
(23) Bäumler, H.; Georgieva, R. Coupled Enzyme Reactions in Multicompartment Microparticles. *Biomacromolecules* **2010**, *11*, 1480−1487.
(24) Lomas, H.; Johnston, A. P. R.; Such, G. K.; Zhu, Z.; Liang, K.; Van Koeverden, M. P.; Alongkornchotikul, S.; Caruso, F. Polymersome-Loaded Capsules for Controlled Release of DNA. *Small* **2011**, *7*, 2109−2019.
(25) Driever, C. D.; Mulet, X.; Johnston, A. P. R.; Waddington, L. J.; Thissen, H.; Caruso, F.; Drummond, C. J. Converging Layer-by-Layer Polyelectrolyte Microcapsule and Cubic Lyotropic Liquid Crystalline Nanoparticle Approaches for Molecular Encapsulation. *Soft Matter* **2011**, *7*, 4257−4266.
(26) Städler, B.; Price, A. D.; Zelikin, A. N. A Critical Look at Multilayered Polymer Capsules in Biomedicine: Drug Carriers, Artificial Organelles, and Cell Mimics. *Adv. Funct. Mater.* **2011**, *21*, 14−28.
(27) Städler, B.; Price, A. D.; Chandrawati, R.; Hosta-Rigau, L.; Zelikin, A. N.; Caruso, F. Polymer Hydrogel Capsules: En Route Toward Synthetic Cellular Systems. *Nanoscale* **2009**, *1*, 68−73.
(28) Hosta-Rigau, L.; Shimoni, O.; Städler, B.; Caruso, F. Advanced Subcompartmentalized Microreactors: Polymer Hydrogel Carriers Encapsulating Polymer Capsules and Liposomes. *Small* **2013**, *9*, 3573−3583.
(29) Bolinger, P.-Y.; Stamou, D.; Vogel, H. An Integrated Self-Assembled Nanofluidic System for Controlled Biological Chemistries. *Angew. Chem., Int. Ed.* **2008**, *47*, 5544−5549.
(30) Kreft, O.; Prevot, M.; Moehwald, H.; Sukhorukov, G. B. Shell-in-Shell Microcapsules: A Novel Tool for Integrated, Spatially Confined Enzymatic Reactions. *Angew. Chem., Int. Ed.* **2007**, *46*, 5605−5608.
(31) Städler, B.; Chandrawati, R.; Price, A. D.; Chong, S.-F.; Breheney, K.; Postma, A.; Connal, L. A.; Zelikin, A. N.; Caruso, F. A Microreactor with Thousands of Subcompartments: Enzyme-Loaded Liposomes within Polymer Capsules. *Angew. Chem., Int. Ed.* **2009**, *48*, 4359−4362.
(32) Chandrawati, R.; Hosta-Rigau, L.; Vanderstraaten, D.; Lokuliyana, S. A.; Städler, B.; Albericio, F.; Caruso, F. Engineering Advanced Capsosomes: Maximizing the Number of Subcompartments, Cargo Retention, and Temperature-Triggered Reaction. *ACS Nano* **2010**, *4*, 1351−1361.
(33) Hosta-Rigau, L.; Chung, S. F.; Postma, A.; Chandrawati, R.; Städler, B.; Caruso, F. Capsosomes with "Free-Floating" Liposomal Subcompartments. *Adv. Mater.* **2011**, *23*, 4082−4087.
(34) Chandrawati, R.; Odermatt, P. D.; Chong, S.-F.; Price, A. D.; Städler, B.; Caruso, F. Triggered Cargo Release by Encapsulated Enzymatic Catalysis in Capsosomes. *Nano Lett.* **2011**, *11*, 4958−4963.
(35) Hosta-Rigau, L.; Chandrawati, R.; Saveriades, E.; Odermatt, P. D.; Postma, A.; Ercole, F.; Breheney, K.; Wark, K. L.; Städler, B.; Caruso, F. Noncovalent Liposome Linkage and Miniaturization of Capsosomes for Drug Delivery. *Biomacromolecules* **2010**, *11*, 3548−3555.
(36) Hosta-Rigau, L.; Städler, B.; Yan, Y.; Nice, E. C.; Heath, J. K.; Albericio, F.; Caruso, F. Capsosomes with Multilayered Subcompartments: Assembly and Loading with Hydrophobic Cargo. *Adv. Funct. Mater.* **2010**, *20*, 59−66.
(37) Wohl, B. M.; Engbersen, J. F. J. Responsive Layer-by-Layer Materials for Drug Delivery. *J. Controlled Release* **2012**, *158*, 2−14.
(38) Sedo, J.; Saiz-Poseu, J.; Busque, F.; Ruiz-Molina, D. Catechol-Based Biomimetic Functional Materials. *Adv. Mater.* **2013**, *25*, 653−701.
(39) Lynge, M. E.; van der Westen, R.; Postma, A.; Städler, B. Polydopamine-a Nature-Inspired Polymer Coating for Biomedical Science. *Nanoscale* **2011**, *3*, 4916−4928.
(40) Lee, H.; Dellatore, S. M.; Miller, W. M.; Messersmith, P. B. Mussel-Inspired Surface Chemistry for Multifunctional Coatings. *Science* **2007**, *318*, 426−430.
(41) Dreyer, D. R.; Miller, D. J.; Freeman, B. D.; Paul, D. R.; Bielawski, C. W. Elucidating the Structure of Poly(dopamine). *Langmuir* **2012**, *28*, 6428−6435.
(42) Della Vecchia, N. F.; Avolio, R.; Alfe, M.; Errico, M. E.; Napolitano, A.; d'Ischia, M. Building-Block Diversity in Polydopamine Underpins a Multifunctional Eumelanin-Type Platform Tunable Through a Quinone Control Point. *Adv. Funct. Mater.* **2013**, *23*, 1331−1340.
(43) Cui, J.; Yan, Y.; Such, G. K.; Liang, K.; Ochs, C. J.; Postma, A.; Caruso, F. Immobilization and Intracellular Delivery of an Anticancer Drug Using Mussel-Inspired Polydopamine Capsules. *Biomacromolecules* **2012**, *13*, 2225−2228.
(44) Ochs, C. J.; Hong, T.; Such, G. K.; Cui, J.; Postma, A.; Caruso, F. Dopamine-Mediated Continuous Assembly of Biodegradable Capsules. *Chem. Mater.* **2011**, *23*, 3141−3143.
(45) Zhu, B.; Edmondson, S. Polydopamine-Melanin Initiators For Surface-Initiated ATRP. *Polymer* **2011**, *52*, 2141−2149.
(46) An, J. H.; Huynh, N. T.; Jeon, Y. S.; Kim, J.-H. Surface Modification Using Bio-Inspired Adhesive Polymers Based On Polyaspartamide Derivatives. *Polym. Int.* **2011**, *60*, 1581−1586.
(47) Zhang, Y.; Thingholm, B.; Goldie, K. N.; Ogaki, R.; Städler, B. Assembly of Poly(dopamine) Films Mixed with a Nonionic Polymer. *Langmuir* **2012**, *28*, 17585−17592.
(48) Tsai, W.-B.; Chien, C.-Y.; Thissen, H.; Lai, J.-Y. Dopamine-Assisted Immobilization of Poly(Ethylene Imine) Based Polymers for Control Of Cell-Surface Interactions. *Acta Biomater.* **2011**, *7*, 2518−2525.
(49) Zhang, Y.; Panneerselvam, K.; Ogaki, R.; Hosta-Rigau, L.; van der Westen, R.; Jensen, B. E. B.; Teo, B. M.; Zhu, M.; Städler, B. Assembly of Poly(dopamine)/Poly(N-isopropylacrylamide) Mixed Films and Their Temperature-Dependent Interaction with Proteins, Liposomes, and Cells. *Langmuir* **2013**, *29*, 10213−10222.
(50) Hosta-Rigau, L.; Zhang, Y.; Teo, B. M.; Postma, A.; Städler, B. Cholesterol—A Biological Compound as a Building Block In Bionanotechnology. *Nanoscale* **2013**, *5*, 89−109.
(51) Postma, A.; Yan, Y.; Wang, Y.; Zelikin, A. N.; Tjipto, E.; Caruso, F. Self-Polymerization of Dopamine as a Versatile and Robust Technique to Prepare Polymer Capsules. *Chem. Mater.* **2009**, *21*, 3042−3044.
(52) Yu, B.; Wang, D. A.; Ye, Q.; Zhou, F.; Liu, W. Robust Polydopamine Nano/Microcapsules and their Loading and Release Behavior. *Chem. Commun.* **2009**, 6789−6791.

(53) Cui, J.; Wang, Y.; Postma, A.; Hao, J.; Hosta-Rigau, L.; Caruso, F. Monodisperse Polymer Capsules: Tailoring Size, Shell Thickness, and Hydrophobic Cargo Loading via Emulsion Templating. *Adv. Funct. Mater.* **2010**, *20*, 1625−1631.
(54) Liu, Q.; Yu, B.; Ye, W.; Zhou, F. Highly Selective Uptake and Release of Charged Molecules by pH-Responsive Polydopamine Microcapsules. *Macromol. Biosci.* **2011**, *11*, 1227−1234.
(55) Zhang, L.; Shi, J.; Jiang, Z.; Jiang, Y.; Qiao, S.; Li, J.; Wang, R.; Meng, R.; Zhu, Y.; Zheng, Y. Bioinspired Preparation of Polydopamine Microcapsule for Multienzyme System Construction. *Green Chem.* **2011**, *13*, 300−306.
(56) Lynge, M. E.; Laursen, M. B.; Hosta-Rigau, L.; Jensen, B. E. B.; Ogaki, R.; Smith, A. A. A.; Zelikin, A. N.; Städler, B. Liposomes as Drug Deposits in Multilayered Polymer Films. *ACS Appl. Mater. Interfaces* **2013**, *5*, 2967−2975.
(57) Chandrawati, R.; Städler, B.; Postma, A.; Connal, L. A.; Chong, S.-F.; Zelikin, A. N.; Caruso, F. Modeling Capsosome Assembly: From Tailor-made Building Blocks to Intact Cargo-loaded Sub-compartmentalized Capsules. *Biomaterials* **2009**, *30*, 5988−5998.
(58) Zelikin, A. N.; Price, A. D.; Städler, B. Poly(Methacrylic Acid) Polymer Hydrogel Capsules: Drug Carriers, Sub-compartmentalized Microreactors, Artificial Organelles. *Small* **2010**, *6*, 2201−2207.
(59) Shi, J.; Zhang, L.; Jiang, Z. Facile Construction of Multi-compartment Multienzyme System through Layer-by-Layer Self-Assembly and Biomimetic Mineralization. *ACS Appl. Mater. Interfaces* **2011**, *3*, 881−889.
(60) Heinig, M.; Johnson, R. J. Role of Uric Acid in Hypertension, Renal Disease, and Metabolic Syndrome. *Clev. Clin. J. Med.* **2006**, *73*, 1059−1064.
(61) Tausche, A. K.; Unger, S.; Richter, K.; Wunderlich, C.; Grassler, J.; Roch, B.; Schroder, H. E. Hyperuricemia and Gout: Diagnosis and Therapy. *Internist* **2006**, *47*, 549−555.
(62) Bhargava, A. K.; Lal, H.; Pundir, C. S. Discrete Analysis of Serum Uric Acid with Immobilized Uricase and Peroxidase. *J. Biochem. Biophys. Methods* **1999**, *39*, 125−136.
(63) Suzuki, M.; Takayanagi, M.; Yashiro, T. Use of the Ortho-Phenylendiamine Fluorescence System in the Enzymatic Assay of Serum-Uric Acid. *Chem. Pharm. Bull.* **1991**, *39*, 2745−2747.
(64) Kayamori, Y.; Katayama, Y.; Urata, T. Nonenzymatic Elimination of Ascorbic Acid in Clinical Samples. *Clin. Biochem.* **2000**, *33*, 25−29.
(65) Martinez-Perez, D.; Ferrer, M. L.; Mateo, C. R. A Reagent Less Fluorescent Sol-Gel Biosensor for Uric Acid Detection in Biological Fluids. *Anal. Biochem.* **2003**, *322*, 238−242.